Iranian Journal of Numerical Analysis and Optimization
Vol. 15, No. 4, 2025, pp 1464–1481
https://doi.org/10.22067/ijnao.2025.94329.1677
https://ijnao.um.ac.ir/

Research Article

Numerical solution of nonlinear diffusion-reaction in porous catalysts using quantum spectral successive linearization method

S. Abbasbandy

Abstract

Significant advances in quantum computing science have been achieved through the development of general-purpose quantum solvers for linear differential equations in several studies. This study employs a hybrid quantum-spectral approach to analyze nonlinear reaction-diffusion dynamics in porous catalysts. Two distinct forms of nonlinearity in the model are examined. The successive linearization method is applied to linearize the governing equations. Within an iterative framework, the final quantum state is constructed by progressively integrating the quantum state from each iteration, enabled by an efficient quantum algorithm. Numerical simulations validate the method's efficacy, showing favorable agreement with existing literature. Moreover, the approach delivers accurate solutions even for large Thiele modulus values.

Received 9 July 2025; revised 16 August 2025; accepted 19 August 2025

Saeid Abbasbandy
Department of Applied Mathematics, Faculty of Science, Imam Khomeini International University, Qazvin, Iran. e-mail: abbasbandy@yahoo.com, abbasbandy@sci.ikiu.ac.ir.

How to cite this article
Abbasbandy, S., Numerical solution of nonlinear diffusion-reaction in porous catalysts using quantum spectral successive linearization method. *Iran. J. Numer. Anal. Optim.*, 2025; 15(4): 1464-1481. https://doi.org/10.22067/ijnao.2025.94329.1677

AMS subject classifications (2020): 65L05, 68Q09, 81P68.

Keywords: Catalyst pellet; Diffusion and reaction; Thiele modulus; Nonlinear reactive transport model.

1 Introduction

Nonlinear phenomena are essential, and many aspects of diffusion and reaction in porous catalysts have been thoroughly investigated. As we know, finding the closed form solution to a problem is very difficult; in many cases, it is impossible to find the solution. In this case, finding semi-analytical or numerical solutions is significant, for example, perturbation methods [34, 38], nonperturbation methods [30], Adomian decomposition method [3, 32], δ-expansion method [23], and homotopy analysis method (HAM) [1, 9, 18, 28].

In recent years, artificial intelligence and deep learning methods have been increasingly applied to compute approximate analytical and semi-analytical solutions for differential equations. Deep learning is a subset of machine learning that utilizes multi-layered artificial neural networks to model complex patterns in data. By automatically extracting hierarchical features—from low-level details to high-level abstractions—deep learning has revolutionized fields such as computer vision, natural language processing, and scientific research. Architectures like convolutional neural networks, recurrent neural networks, and transformers power applications ranging from image recognition and autonomous driving to language translation and drug discovery. While its success relies on large datasets and significant computational resources, advancements in efficiency (e.g., lightweight models, federated learning) and interpretability continue to expand its potential. Despite challenges like overfitting and ethical concerns, deep learning remains at the forefront of artificial intelligence, driving innovations that reshape industries and everyday life, [16, 17, 15].

The study of coupled diffusion and reaction in porous catalysts is an important topic in chemical engineering, as it involves a nonlinear problem. Thiele [39] derived an analytical solution for first-order reactions; for higher-order reactions and further details, see [5, 33, 35]. The HAM was employed

by Abbasbandy [1] to investigate the nonlinear coupled diffusion-reaction dynamics in porous catalysts. The steady-state reactive transport model (RTM) was recently studied by Ganie et al. [19], generalizing nonlinear reaction-diffusion dynamics in porous catalysts for micro-vessel applications. We study their examples in this article. While many numerical methods address nonlinear problems in heat transfer, fluid dynamics, and chemical reactors, their accuracy often hinges on reaction rates and initial conditions, precluding the derivation of series solutions.

Several studies have designed general-purpose quantum solvers for linear differential equations, achieving notable advances in quantum oracle complexity. For global numerical differentiation methods, in [2, 11], it was introduced a spectral-based solver by using the Chebyshev polynomials of the first kind. As established by the Remez algorithm [161,162], Chebyshev polynomials provide an optimal basis for L_∞-norm approximation [26].

We present a quantum algorithm for solving linear ordinary differential equations (ODEs) using spectral methods—a global approximation technique that contrasts with finite difference approaches. Our method efficiently handles time-dependent initial and boundary value problems with favorable computational complexity. Quantum computing has seen growing interest in solving differential equations. For instance, Leyton and Osborne [27] introduced a quantum Euler method for nonlinear ODEs with polynomial nonlinearities, achieving logarithmic complexity in system dimension but exhibiting exponential scaling in evolution time (a fundamental limitation for general nonlinear ODEs). Other advances focus on partial differential equations (PDEs). Clader, Jacobs, and Sprouse [12] employed the quantum linear systems algorithm (QLSA) in a finite element method for Maxwell's equations, while Costa, Jordan, and Ostrander [13] leveraged Hamiltonian simulation for finite difference approximations of the wave equation. More recently, Arrazola et al. [6] proposed a continuous-variable quantum algorithm for nonhomogeneous linear PDEs in initial value problems (IVPs).

This article presents a quantum pseudo-spectral method (QPSM) for solving the nonlinear diffusion-reaction model in porous catalysts [1, 19]. The governing equations consist of nonlinear second-order differential equations subject to boundary value problems (BVPs). The application of QPSM to

linear IVPs via the QLSA was first presented in [11]. Subsequent work in [2] has demonstrated its effectiveness for Lane–Emden type equations. The QLSA for a linear sparse system of d equations produces a quantum state proportional to the solution system in time poly(log d), and it is improved in [10]. Berry [7] developed a quantum algorithm employing finite difference schemes to solve general linear ODEs, demonstrating poly$(1/\epsilon)$ complexity relative to solution accuracy ϵ. Later, the complexity is improved to poly(log$(1/\epsilon)$) in [8]. The quantum algorithm in [11] is based on a pseudo-spectral method for time-dependent IVP and BVP with the complexity poly(log d, log$(1/\epsilon)$). Newly, by using Carleman linearization, the nonlinear quadratic ODEs are considered by a quantum algorithm with complexity E^2q poly(log E; log d; log $1/\epsilon)/\epsilon$, where E is the evolution time and q measures decay of the solution, [14, 25, 29].

Our analysis focuses on solving the governing equation for a one-dimensional steady-state reactive model:

$$\frac{\mathrm{d}^2u}{\mathrm{d}x^2} - \varphi^2 u^N = 0, \qquad x \in [0,1], \tag{1}$$

and the boundary conditions

$$\frac{\mathrm{d}u}{\mathrm{d}x}\Big|_{x=0} = 0, \qquad u(1) = 1, \tag{2}$$

where φ is Thiele modulus [31, 39] and N is the order reaction. The successive linearization method (SLM) is first employed, as QPSM demonstrates particular efficiency for linear systems. Hence we have a hybrid quantum spectral successive linearization method (QSSLM). We consider an expansion of the unknown function $u(\cdot)$ in the form:

$$u(\tau) = U_i(\tau) + \sum_{k=0}^{i-1} u_k(\tau), \qquad i = 1, 2, 3, \ldots. \tag{3}$$

Let $U_i(\cdot)$ denote the unknown functions and let $u_k(\cdot)$ be their successive approximations. The latter are obtained via QPSM, which solves the linearized version of the original equation—obtained by inserting (3) into (1)—in a recursive manner. Applying (3) in (1) by considering the Binomial theorem,

we have

$$U_i'' - \varphi^2 \sum_{l=0}^{N} \binom{N}{l} U_i^{N-l} \Big(\sum_{j=0}^{i-1} u_j\Big)^l = -\sum_{j=0}^{i-1} u_j''. \tag{4}$$

We choose the constant function $u_0(\cdot) = 1$ as our initial approximation, which satisfies the boundary conditions specified in (2). Also, we assume that $\lim_{i\to\infty} U_i = 0$. For $i \geq 1$, each $u_i(\cdot)$ is determined by solving the linear IVP resulting from the linearization of (4) for $i \in [M] = \{1, 2, 3, \ldots, M\}$:

$$u_i'' - \varphi^2 N b_{i-1}^{N-1} u_i = \mu_{i-1}, \tag{5}$$

where

$$\begin{aligned} b_{i-1}(\cdot) &= \sum_{j=0}^{i-1} u_j(\cdot), \\ \mu_{i-1}(\cdot) &= -b_{i-1}''(\cdot) + \varphi^2 b_{i-1}^N(\cdot). \end{aligned}$$

The solutions $u_{i\geq 1}(\cdot)$ satisfy the initial conditions $u_i(0) = 0$ and $u_i'(0) = 0$, where M denotes the number of iterations. Prior to applying the quantum spectral method, we first transform the IVP (5) into an equivalent system of first-order ODEs:

$$\begin{aligned} y_{i,0}'(x) &= y_{i,1}(x), \\ y_{i,1}'(x) &= \mu_{i-1}(x) + \varphi^2 N b_{i-1}^{N-1}(x) y_{i,0}(x).. \end{aligned} \tag{6}$$

This system satisfies $y_{i,0}(0) = y_{i,1}(0) = 0$, where $y_{i,0} = u_i$ and $y_{i,1} = u_i'$. Following (6), consider the coefficient matrix as follows:

$$A_i(\cdot) = \begin{bmatrix} 0 & 1 \\ \varphi^2 N b_{i-1}^{N-1}(\cdot) & 0 \end{bmatrix}.$$

The spectral approach represents solutions as linear combinations of orthogonal polynomials (typically Chebyshev), with differential equations transformed to algebraic equations through pseudo-spectral discretization at the Gauss–Lobatto nodes [37]. Applying this framework, we employ a truncated Chebyshev expansion within the Chebyshev pseudo-spectral method [22] to

(5), yielding:

$$u_i(\cdot) = \sum_{j=0}^{n} c_{i,j} T_j(\cdot), \tag{7}$$

for any $n \in \mathbb{Z}^+$ and Chebyshev polynomials, $T_j(\cdot)$. Consistent with Chebyshev polynomial theory, we work on $[-1, 1]$ in (7) and accordingly rescale (1). The numerical solution utilizes Chebyshev–Gauss–Lobatto collocation points $\xi_l = \cos(\frac{l\pi}{n})$ for $l \in [n+1]_0 = \{0, 1, \ldots, n\}$ to discretize the linear system obtained from (5). For computing $c_{i,k}$, we have

$$\frac{\mathrm{d}u_i(\xi)}{\mathrm{d}\xi} = \sum_{k=0}^{n} \sum_{j=0}^{n} [D_n]_{k,j} c_{i,j} T_k(\xi),$$

where the matrix D_n is defined in [40]. Using (6) and (7), for $i \in [M]$ and $l \in [n+1]_0$, we have

$$\begin{aligned} \sum_{j=0}^{n} T_j(\xi_l) c'_{i,0,j} &= \sum_{j=0}^{n} T_j(\xi_l) c_{i,1,j}, \\ \sum_{j=0}^{n} T_j(\xi_l) c'_{i,1,j} &= \mu_{i-1} + \varphi^2 N b_{i-1}^{N-1}(\xi_l) \sum_{j=0}^{n} c_{i,0,j} T_j(\xi_l), \end{aligned} \tag{8}$$

where $c_{i,l,\cdot}$ and $c'_{i,l,\cdot}$ are Chebyshev coefficients related to functions $y_{i,l}(\cdot)$ and $y'_{i,l}(\cdot)$ for $l = 0, 1$, respectively. The linear system (8) is solved by the QLSA [10], which achieves a complexity of poly$(\log 2)$. The convergence properties of this approach are supported by theoretical results from [11, 20]. Specifically, we have the following properties:

- If $u \in C^{r+1}(-1, 1)$, then the error norm scales as $\mathcal{O}(n^{2-r})$.
- For $u \in C^{\infty}(-1, 1)$, then the error norm exhibits spectral convergence, scaling as $\sqrt{\frac{2}{\pi}}(\frac{e}{2n})^n$.

In the latter case, selecting $n = \text{poly}(\log(1/\epsilon))$ ensures an ϵ-approximation of the solution. In solving IVPs, to improve the accuracy, we usually divide the region including the independent variable into some subintervals. Indeed here, we want to solve a BVP, and hence, we cannot do this. Hence, by increasing the values of n and M, we improve the accuracy. For using the Chebyshev polynomials, we should convert $[0, 1]$ in (1) to $[-1, 1]$. After this,

$x \in [0,1]$ converts to $\xi \in [-1,1]$ by $\xi = K(x) = 1 - 2x$, and conversely, $x = IK(\xi) = \frac{(1-\xi)}{2}$. Hence, (6) converts to

$$\begin{aligned} z'_{i,0}(\xi) &= z_{i,1}(\xi), \\ z'_{i,1}(\xi) &= \eta_{i-1}(\xi) + \varphi^2 \frac{N}{D^2} b_{i-1}^{N-1}(\xi) z_{i,0}(\xi), \end{aligned} \tag{9}$$

where

$$\begin{aligned} b_{i-1}(\cdot) &= \sum_{j=0}^{i-1} z_{j,0}(\cdot), \\ \eta_{i-1}(\cdot) &= -\Big(b''_{i-1}(\cdot) - \varphi^2 \frac{1}{D^2} b_{i-1}^{N}(\cdot) \Big), \end{aligned}$$

and $D = \frac{\mathrm{d}\xi}{\mathrm{d}x}$ and $z_{i,v}(\xi) = y_{i,v}(\xi) = y_{i,v}(IK_h(\xi))$ for $\xi \in [0,1]$, $i \in [M]$ and $v \in \{0,1\}$. For convenience, we set $z_{0,0} = 1$ and consequently $z_{0,1} = 0$. Following (9), we have

$$A_i(\xi) = \begin{bmatrix} 0 & 1 \\ \frac{N\varphi^2}{D^2} b_{i-1}^{N-1}(\xi) & 0 \end{bmatrix}.$$

2 Quantum implementation

For a better understanding of quantum computing symbols, see [41]. Here, we analyze the linear system

$$L_i |X_i\rangle = |B_i\rangle, \tag{10}$$

derived from the previous section. Using quantum computations applied to (9), we solve this system to obtain approximate solutions at the terminal point $x = 1$ for each iteration $i \in [M]$. The vector $|X_i\rangle \in \mathbb{C}^{p+2} \otimes \mathbb{C}^2 \otimes \mathbb{C}^{n+1}$ describes the solution by

$$|X_i\rangle = \sum_{v=0}^{1} \sum_{j=0}^{n} c_{i,v,j} |0vj\rangle + \sum_{h=1}^{p+1} \sum_{v=0}^{1} \sum_{j=0}^{n} x_{iv} |hvj\rangle. \tag{11}$$

The coefficient $c_{i,\upsilon,l}$ expands $z_{i,\upsilon}(K(1))$ in Chebyshev series, while $x_{i\upsilon} = z_{i,\upsilon}(K(0))$ gives the final state. The padding parameter p [21, 8] amplifies the solution for reliable quantum measurement. Thus, the solution at $x = 1$ (the final state) is given by $1 + \sum_{i=1}^{M} x_{i1}$, where the constant term accounts for the initial approximation $u_0(\cdot) = 1$.

In (1),

$$|B_i\rangle = \sum_{\upsilon=0}^{1} 0|\upsilon 0\rangle + \sum_{j=1}^{n} 0|0j\rangle + \sum_{j=1}^{n} \eta_{i-1}(\xi_j)|1j\rangle,$$

and

$$\begin{aligned} L_i = {} & |0\rangle\langle 0| \otimes (L1 + L2(A_i)) + |1\rangle\langle 0| \otimes L3 \\ & + \sum_{h=1}^{p+1} |h\rangle\langle h| \otimes L4 + \sum_{h=1}^{p+1} |h\rangle\langle h-1| \otimes L5. \end{aligned}$$

The matrix $L1$ is a discrete representation for derivative process; that is,

$$|0\rangle\langle 0| \otimes L1|X_i\rangle = \sum_{\upsilon=0}^{1}\sum_{k=0}^{n} T_k(\xi_0)c_{i,\upsilon,k}|0\upsilon 0\rangle + \sum_{\upsilon=0}^{1}\sum_{j=1,k,r=0}^{n} T_k(\xi_j)[D_n]_{k,r}c_{i,\upsilon,r}|0\upsilon j\rangle,$$

and hence

$$\begin{aligned} L1 &= \sum_{\upsilon=0}^{1}\sum_{k=0}^{n} T_k(\xi_0)|\upsilon 0\rangle\langle \upsilon k| + \sum_{\upsilon=0}^{1}\sum_{j=1,k,r=0}^{n} \cos\frac{kj\pi}{n}[D_n]_{k,r}|\upsilon j\rangle\langle \upsilon r| \\ &= I_2 \otimes \Big(|0\rangle\langle 0|P_n + \sum_{j=1}^{n} |j\rangle\langle j|P_n D_n\Big), \end{aligned}$$

where

$$P_n = \sum_{j,k=0}^{n} \cos\frac{kj\pi}{n}|j\rangle\langle k|.$$

The matrix $L2(A_i)$ discretizes $A_i(\xi)$ as follows:

$$|1\rangle\langle 1| \otimes L2(A_i)|X_i\rangle = -\sum_{\upsilon,\varrho=0}^{1}\sum_{j=1,k=0}^{n} A_i(\xi_j)_{\upsilon,\varrho}T_k(\xi_j)c_{i,\varrho,k}|1\upsilon j\rangle,$$

and then

$$L2(A_i) = -\sum_{v,\varrho=0}^{1}\sum_{j=1,k=0}^{n} A_i(\xi_j)_{v,\varrho}\cos\frac{kj\pi}{n}|vj\rangle\langle\varrho k| = -\sum_{j=1}^{n} A_i(\xi_j)\otimes|j\rangle\langle j|P_n.$$

In practice, the Chebyshev coefficients in $L3$ are chosen to ensure patchwise continuity; that is, the endpoint of one subinterval $z_{i,h}(-1)$ aligns with the start of the next $z_{i,h+1}(1)$,

$$L3 = -\sum_{k=0}^{n}(-1)^k|0\rangle\langle k|.$$

The matrices $L3$ and $L4$ optimize the success probability of the final quantum measurement. Specifically, $L4$ processes the output of $L3$ (for $l = 0$) to construct x_{iv}, iterating this operation n times across all $l \in [n]$. Hence $L3$ and $L4$ repeat x_{iv}, $(n+1)p$ times for $l \in [n]$, and then for an artificial parameter h, we have

$$L3 = -\sum_{k=0}^{n}(-1)^k|0\rangle\langle k|,$$

$$L4 = -\sum_{\upsilon=0}^{1}\sum_{j=1}^{n}|\upsilon j\rangle\langle\upsilon(j-1)| + \sum_{\upsilon=0}^{1}\sum_{j=0}^{n}|\upsilon j\rangle\langle\upsilon j|,$$

and

$$L5 = -\sum_{\upsilon=0}^{1}|\upsilon 0\rangle\langle\upsilon n|.$$

Remark 2.1. Because of the boundary condition $u(1) = 1$ in (2), we have $\xi_0 \leftrightarrow \xi_n$ in constructing $L1$.

3 Numerical results

Here, we examine several examples with varying values of φ and N in (1) to demonstrate the method's accuracy and compare it with other approaches. All computations are performed using Python 3.12.4 on a DESKTOP with

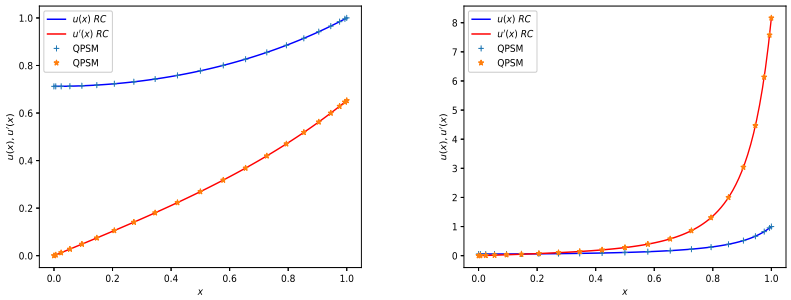

Figure 1: Comparison for $N = 2$, $\varphi = 1(Left)$, $\varphi = 10(Right)$: $(n = 20, M = 10)$.

Intel(R) Core(TM) i7-7700 CPU with 8.00 GB RAM, and for simplicity, we set $p = 1$ in every case. We consider only the nonlinear case in the following examples in [1] and illustrate the results for $N = 0.5, 2, 4$ for various φ. For comparison, we consider the numerical method based on residual control (RC) [24] and HAM [1] and the finite difference method (FDM) based on the three-stage Lobatto formula with fourth-order accuracy for C^1-continuous solution [36]. Figures 1, 2, and 3 show $u(\cdot)$ and $u'(\cdot)$ for QPSM (present method) and others. Figure 4 shows the residual errors in (1), which show the efficiency of QPSM. Only in Figure 3, the obtained results by RC are not fine, and for this reason, we compare QPSM with the HAM solution. Table 1 shows a comparison between QPSM with $n = 20$ and $M = 10$ (for $\varphi \geq 10$, we put $n = 30$) and other methods. In this table, the results for $\varphi = 0.5$ in RC are not fine. The last column of Table 1 presents the CPU time in seconds, which is remarkably small and noteworthy.

4 The reactive transport model

We will consider the RTM (reactive transport model) dynamics with the variance in the half-saturation concentration, α, and the characteristic reaction rate, β, as follows [4, 19]:

$$\frac{\mathrm{d}^2 u}{\mathrm{d}x^2} - \frac{\beta u(x)}{\alpha + u(x)} = 0, \qquad x \in [0, 1], \tag{12}$$

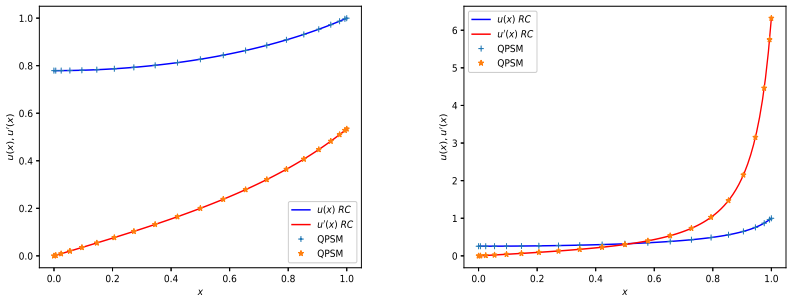

Figure 2: Comparison for $N = 4,\ \varphi = 1(Left),\ \varphi = 10(Right)$: $(n = 20, M = 10)$.

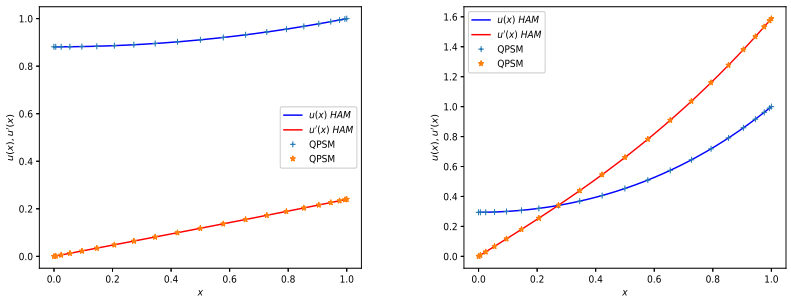

Figure 3: The Comparison for $N = 0.5,\ \varphi = 0.5(Left),\ \varphi = 1.5(Right)$: $(n = 20, M = 10)$.

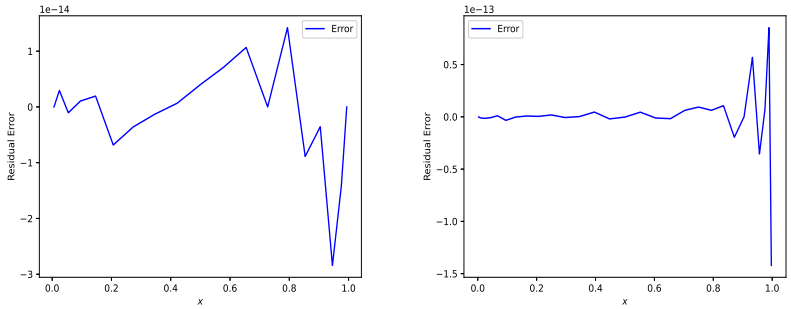

Figure 4: Residual error for $N = 2, (Left),\ N = 4(Right)$: $(\varphi = 10, n = 20, M = 10)$.

Table 1: Results for $u(0)$ at various values of N and φ.

N	φ	QPSM	HAM	FDM	RC	CPU Time (QPSM)
0.5	0.5	0.88135825	0.881358	0.881359	–	0.43
0.5	1	0.59444614	0.594446	0.594447	–	0.43
0.5	1.5	0.29428991	0.294290	0.294290	–	0.43
2	1	0.71225634	0.712256	0.712257	0.712256	0.30
2	2	0.44372272	0.443723	0.443723	0.443723	0.29
2	4	0.21259027	0.212590	0.212591	0.212590	0.29
2	10	0.057084208	0.0570842	0.0570843	0.0570842	0.42
2	20	0.017555306	0.0175553	0.0175615	0.0175553	0.29
4	1	0.779145162	0.779145	0.779148	0.779146	0.75
4	10	0.257002936	0.257003	0.257005	0.257002	0.75

and the boundary conditions (2); that is, $u'(0) = 0,\ u(1) = 1$.

In this case after linearization, (9) converts to

$$\begin{aligned} z'_{i,0}(\xi) &= z_{i,1}(\xi), \\ z'_{i,1}(\xi) &= \eta_{i-1}(\xi) + \frac{1}{D^2}\frac{\beta\alpha}{(\alpha + b_{i-1}(\xi))^2} z_{i,0}(\xi), \end{aligned} \tag{13}$$

where

$$\begin{aligned} b_{i-1}(\cdot) &= \sum_{j=0}^{i-1} z_{j,0}(\cdot), \\ \eta_{i-1}(\cdot) &= -\Big(b''_{i-1}(\cdot) - \frac{1}{D^2}\frac{\beta b_{i-1}(\cdot)}{\alpha + b_{i-1}(\cdot)}\Big), \end{aligned}$$

and hence the matrix of coefficients is

$$A_i(\xi) = \begin{bmatrix} 0 & 1 \\ \frac{1}{D^2}\frac{\beta\alpha}{(\alpha+b_{i-1}(\xi))^2} & 0 \end{bmatrix}.$$

Figure 5 shows a comparison between QPSM and RC for $n = 20$ and $M = 5$ for different values of α and β. These values for α and β are chosen from [19] for better comparison, the system of (13) is independent of the values of α and β. In Table 2, QPSM is compared with the Runge–Kutta method (RK4), particle swarm optimization (PSO), and a hybrid of PSO-sequential quadratic programming (PSO-SQP) [19]. In this table, we report only the values of $u(0)$ because it is a missed value and important.

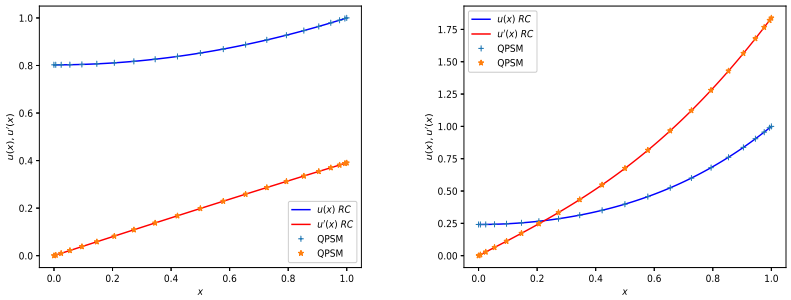

Figure 5: Comparison for $\alpha = -0.2, \beta = 0.3(Left)$, $\alpha = 1, \beta = 6(Right)$: $(n = 20, M = 5)$.

Table 2: Results for $u(0)$ at various values of α and β.

α	β	QPSM	RK4	PSO	PSO-SQP
0.2	0.5	0.7985197734	0.798520	0.798521	0.798520
-0.2	0.3	0.8026489484	0.802648942	0.802647404	0.802648945
1	6	0.2412718196	0.241272	0.241277	0.241272

5 Conclusions

This paper introduced a new method for solving the nonlinear diffusion-reaction model in porous catalysts, with potential applications in soft tissues and microvessels, using a QPSM. These highly nonlinear models were treated using the SLM to convert the governing equations into a linearized form. Comparative studies with numerical and semi-analytical methods demonstrated the efficiency of the proposed approach. By selecting appropriate parameter values, the method yields highly accurate results. Results showed consistent advantages in speed and accuracy over prior work. Although the initial guess represents a critical step in the linearization method for solving nonlinear problems. Future research will explore extensions to high-order fractional differential equations and alternative QPSM collocation schemes.

Acknowledgements: We thank the anonymous reviewers for helpful comments, which lead to definite improvement in the manuscript.

Declarations

Conflict of Interest: The author declares that has no conflict of interest.

Funding: The author declares that this research received no grant from any funding agency in the public, commercial, or not-for-profit sectors.

Competing interests: The author declares that has no conflict of interest.

Data availability: Our manuscript has no associated data.

References

[1] Abbasbandy, S., *Approximate solution for the nonlinear model of diffusion and reaction in porous catalysts by means of the homotopy analysis method,* Chem. Eng. J., 136 (2008) 144–150.

[2] Abbasbandy, S., *Series and rational solutions of the second kind Painlevé equations by using quantum pseudo-spectral method,* Int. J. Math. Math. Sci. 2025 (2025) 9705701.

[3] Adomian G., *Solving frontier problems of physics: The decomposition method,* Kluwer Academic, Dordrecht, 1994.

[4] Ahmad, I., Ilyas, H., Urooj, A., Aslam, M.S., Shoaib, M. and Raja, M.A.Z., *Novel applications of intelligent computing paradigms for the analysis of nonlinear reactive transport model of the fluid in soft tissues and microvessels,* Neural Comput. Appl., 31 (2019) 9041–9059.

[5] Aris, R., *Mathematical theory of diffusion and reaction in permeable catalyst,* Oxford University Press, London, 1975.

[6] Arrazola, J.M., Kalajdzievski, T., Weedbrook, C. and Lloyd, S., *Quantum algorithm for nonhomogeneous linear partial differential equations,* Phys. Rev. A 100 (2019) 032306.

[7] Berry, D.W., *High-order quantum algorithm for solving linear differential equations,* J. Phys. A 47(10) (2014) 105301.

[8] Berry, D.W., Childs, A.M., Ostrander, A. and Wang, G., *Quantum algorithm for linear differential equations with exponentially improved dependence on precision,* Commun. Math. Phys. 356(3) (2017) 1057–1081.

[9] Biazar, J., Dehghan, M., Houlari, T., *Using homotopy analysis method to find the eigenvalues of higher order fractional Sturm–Liouville problems,* Iran. J. Numer. Anal. Optim. 10(1) (2020) 49–62.

[10] Childs, A.M., Kothari, R. and Somma, R.D., *Quantum linear systems algorithm with exponentially improved dependence on precision,* SIAM J. Comput. 46 (2017) 1920–1950.

[11] Childs, A.M. and Liu, J.P., *Quantum spectral methods for differential equations,* Commun. Math. Phys. 375 (2020) 1427–1457.

[12] Clader, D.B., Jacobs, B.C. and Sprouse, C.R., *Preconditioned quantum linear system algorithm,* Phys. Rev. Lett. 110 (2013) 250504.

[13] Costa, P., Jordan, S. and Ostrander, A., *Quantum algorithm for simulating the wave equation,* Phys. Rev. A 99 (2019) 012323.

[14] Costa, P.C.S., Schleich, P., Morales, M.E.S. and Berry, D.W., *Further improving quantum algorithms for nonlinear differential equations via higher-order methods and rescaling,* Npj Quantum Inf. 11 (1) (2025) 141.

[15] Dana Mazraeh, H. and Parand, K., *GEPINN: An innovative hybrid method for a symbolic solution to the Lane–Emden type equation based on grammatical evolution and physics-informed neural networks,* Astron. Comput. 48 (2024) 100846.

[16] Dana Mazraeh, H. and Parand, K., *A three-stage framework combining neural networks and Monte Carlo tree search for approximating analytical solutions to the Thomas–Fermi equation,* J. Comput. Sci. 87 (2025) 102582.

[17] Dana Mazraeh, H. and Parand, K., *An innovative combination of deep Q-networks and context-free grammars for symbolic solutions to differential equations,* Eng. Appl. Artif. Intell. 142 (2025) 109733.

[18] Derakhshan, M. and Aminataei, A., *Comparison of homotopy perturbation transform method and fractional Adams–Bashforth method for the Caputo–Prabhakar nonlinear fractional differential equations,* Iran. J. Numer. Anal. Optim. 10(2) (2020) 63–85.

[19] Ganie, A.H., Rahman, I.U., Sulaiman, M. and Nonlaopon, K., *Solution of nonlinear reaction-diffusion model in porous catalysts arising in microvessel and soft tissue using a metaheuristic,* IEEE Access, 10 (2022) 41813–41827.

[20] Gheorghiu, C.I., *Spectral methods for differential problems,* Casa Cartii de Stiinta Publishing House, Cluj-Napoca, 2007.

[21] Harrow, A.W., Hassidim, A. and Lloyd, S., *Quantum algorithm for linear systems of equations,* Phys. Rev. Lett. 103 (2009) 150502.

[22] Hosseini, M.M., *A modified pseudospectral method for numerical solution of ordinary differential equations systems,* Appl. Math. Comput. 176(2) (2006) 470–475.

[23] Karmishin, A.V., Zhukov, A.I. and Kolosov, V.G., *Methods of dynamics calculation and testing for thin-walled structures,* Mashinostroyenie, Moscow, 1990.

[24] Kierzenka, J. and Shampine, L.F., *A BVP solver based on residual control and the MATLAB PSE,* ACM Trans. Math. Software. 27 (2001) 299–316.

[25] Krovi, H., *Improved quantum algorithms for linear and nonlinear differential equations,* Quantum 7 (2023) 913.

[26] Kyriienko, O., Paine, A.E. and Elfving, V.E., *Solving nonlinear differential equations with differentiable quantum circuits,* Phys. Rev. A, 103(5) (2021) 052416.

[27] Leyton, S.K. and Osborne, T.J., *A quantum algorithm to solve nonlinear differential equations,* arXiv:0812.4423 (2008).

[28] Liao, S.J., *Beyond perturbation: Introduction to the homotopy analysis method,* Chapman and Hall/CRC Press, Boca Raton, 2003.

[29] Liu, J.P., An, D., Fang, D., Wang, J., Low, G.H. and Jordan, S., *Efficient quantum algorithm for nonlinear reaction-diffusion equations and energy estimation,* Commun. Math. Phys. 404 (2023) 963–1020.

[30] Lyapunov, A.M., *General problem on stability of motion* (English translation), Taylor and Francis, London, 1992.

[31] Magyari, E., *Exact analytical solution of a nonlinear reaction–diffusion model in porous catalysts,* Chem. Eng. J. 143 (2008) 167–171.

[32] Mirhosseini-Alizamini, S., *Solving linear optimal control problems of the time-delayed systems by Adomian decomposition method,* Iran. J. Numer. Anal. Optim. 9(2) (2019) 165–183.

[33] Moitsheki, R.J., Hayat, T., Malik, M.Y. and Mahomed, F.M., *Symmetry analysis for the nonlinear model of diffusion and reaction in porous catalysts,* Nonlinear Anal. Real World Appl. 11 (2010) 3031–3036.

[34] Nayfeh, A.H., *Perturbation methods,* John Wiley and Sons, New York, 2000.

[35] Satterfield, C.N., *Mass transfer in heterogeneous catalysis,* MIT Press, Cambridge, 1970.

[36] Shampine, L.F., Reichelt, M.W. and Kierzenka, J., *Solving boundary value problems for ordinary differential equations in MATLAB with bvp4c*, MATLAB File Exchange, 2004.

[37] Shen, J., Tang, T., Wang, L.L., *Spectral methods: Algorithms, analysis and applications,* Springer, Berlin, 2011.

[38] Srinivas, E., Lalu, M. and Phaneendra, K., *A numerical approach for singular perturbation problems with an interior layer using an adaptive spline,* Iran. J. Numer. Anal. Optim. 12(2) (2022) 355–370.

[39] Thiele, E.W., *Relation between catalytic activity and size of particle,* Ind. Eng. Chem. 31 (1939) 916–920.

[40] Trefethen, L.N., *Spectral methods in MATLAB,* Society for Industrial and Applied Mathematics (SIAM), 2000.

[41] Zygelman, B., *A first introduction to quantum computing and information,* Springer Nature Switzerland AG, 2018.